NANO LETTERS

2007
Vol. 7, No. 11
3290−3295

Synchronous Photoluminescence Intermittency (Blinking) along Whole Semiconductor Quantum Wires

John J. Glennon, Rui Tang, William E. Buhro,* and Richard A. Loomis*

Department of Chemistry and Center for Materials Innovation, Washington University in St. Louis, One Brookings Drive, CB 1134, Saint Louis, Missouri 63130

Received June 19, 2007; Revised Manuscript Received August 15, 2007

ABSTRACT

Photoluminescence microscopy studies have detected synchronous-photoluminescence-intensity fluctuations along entire cadmium selenide quantum wires under continuous illumination. While similar photoluminescence blinking has been reported previously for semiconductor quantum dots and rods, the observation of synchronous blinking spanning the entire length of quantum wires, with diameters ≈9 nm and lengths >5 μm, is remarkable. We propose a mechanism to account for the synchronous blinking that is based on a dynamic, photolytic filling of surface-trap sites.

The large absorption cross sections, the direct band gaps throughout the visible and near-infrared spectral regions, and the ease of synthesis of semiconductor nanocrystals have led to efforts aimed at increasing the efficiency of photovoltaic devices by incorporating several types of nanostructured semiconductors. Numerous groups have already shown the promise for incorporating semiconductor quantum dots, QDs, and quantum rods, QRs, in photovoltaic devices.[1−3] The inefficient hopping of charge from the QDs to the conductive polymer film in which the QDs are embedded and from the QDs to other QDs is believed to be a limiting factor in the utility of such devices. One-dimensional nanostructures, or nanowires, represent the smallest structures that can in principle efficiently transport charge along prescribed pathways, and thus information in nanoelectronics.[4] Furthermore, the absorption cross sections of semiconductor nanowires are up to 8× higher per unit volume than those of the widely studied QDs,[5] making them especially attractive for integration into photonics and solar cells.[6]

The vast majority of nanowires reported in the literature, however, lack some of the essential properties of chemically prepared semiconductor colloidal QDs that are required for developing more efficient photovoltaics; mainly, most nanowires do not have the tunability of the band gap absorption and emission energies that arise from controlling the size of the semiconductor near or below the dimensions of twice the exciton Bohr radius where quantum-confinement effects become important.[1,4] Additionally, most syntheses do not produce defect-free nanowires with uniform surface passivation that would enable efficient transport of charge along the nanowires.

We have previously synthesized semiconductor nanowires with diameters as small as 3.5 nm and with lengths up to tens of micrometers by the solution−liquid−solid, SLS, method.[7−9] The details of the synthesis are provided in Supporting Information. These CdSe nanowires exhibit quantum-confinement effects and are hereafter referred to as quantum wires, QWs. We have shown that the dependence of the change in the band gap energy, ΔE_g, which results from quantum confinement, on the diameter of the QWs, d, follows a simple particle-in-a-cylinder quantum-mechanical expression, $\Delta E_g \propto d^{-2}$, where d is the diameter of the QW.[7,8] Cadmium selenide is a direct band gap semiconductor that has a bulk exciton Bohr radius of 5.6 nm,[10] and the quantum confinement arises when the diameter of the QW $< \approx 11$ nm.[7]

Although varying levels of theory can be used to treat the Coulomb and quantum-confinement energies of the electron−hole pairs within the QWs, the total exciton wave function is most often written as a product of wave functions representing the electron, the hole, and the exciton motion along the QW.[11−13] In Cartesian coordinates the total exciton wave function can be written as $\Psi(x_e,y_e,x_h,y_h,z,Z) = \psi_e(x_e,y_e)\psi_h(x_h,y_h)\phi(z)e^{\pm iKZ}$, with Z and $z = z_e - z_h$ representing the position of the center of mass of the exciton and the distance between the positions of the electron and hole along the length of the QW, respectively.[11] Since the Coulomb energy is much weaker than the single particle confinement energy in the radial dimension of the QW, the single-particle states for the electron and hole, $\psi_e(x_e,y_e)$ and $\psi_h(x_h,y_h)$, can

* To whom correspondence should be addressed. E-mail: burho@wustl.edu (W.E.B.); loomis@wustl.edu (R.A.L.).

10.1021/nl0714583 CCC: $37.00
Published on Web 10/10/2007

be approximated using a circular quantum well with a barrier height determined by the electron affinity. Consequently, there is quantum confinement in the radial coordinate of the QWs that shifts the excitonic states toward higher energy with decreasing QW diameter. The wave function of the electron−hole interaction along the length of the QW, $\phi(z)$, is not perturbed and directly results from the Coulomb interaction. Additionally, the exciton has a wave number K determined by the energy of the exciton, and it behaves as a free particle with no restrictions along the length of the QW. Consequently, there is an equal probability of finding an exciton anywhere along an ideal semiconductor QW that has no significant changes or irregularities in the exciton potential.

Photoluminescence images of single CdSe QWs were obtained as a function of time using a commercial fluorescence microscopy apparatus and continuous illumination accessing energies well above the band gap of the QWs. Most of the QWs are dim, indicating a low PL quantum yield, Φ, $<1\%$. A slight increase in the PL intensity is observed with continued irradiation that is consistent with a reversible photoenhancement process.[14] Some of the QWs exhibit intensity twinkling at random positions along the QWs, as has been reported previously.[15] Most often the spatial extent of this localized twinkling is determined by the spatial resolution of the apparatus, ≈300 nm. During these twinkling events, the PL intensity jumps from a state with a low Φ, $<1\%$, to an intense state with $\Phi > 15\%$ within the temporal resolution of the apparatus, >1 ms. Similar PL blinking between somewhat binary "on" and "off" intensity levels has been reported for semiconductor QDs[10,16−26] and QRs[27] and has received significant experimental and theoretical attention.

Somewhat surprisingly, the time-dependent data reveal that with continuous illumination a fraction of the CdSe QWs, typically <2%, begin to exhibit dramatic fluctuations in the PL intensity spanning the entire lengths of the QWs. A detailed analysis of the kinetics for this induction period is problematical since only a small fraction of the QWs exhibit this behavior. Furthermore, it is necessary to illuminate the sample while optimizing the conditions for data acquisition, thus making an accurate induction time difficult to establish. Nevertheless, once the fluctuations begin, typically after a duration of 10−40 s when using excitation power densities between 7 and 100 W cm^{-2}, they have been observed to continue blinking for >1 h. During these fluctuations, the PL intensity is observed to vary between "dark" intensity levels with $\Phi < 1\%$ and "bright" levels with Φ increasing to varying levels up to ≈20%. While the PL intensity spanning a single blinking QW may not be uniform, the intensity is observed to vary synchronously along the entire QW by the same percentage within the time bin of the image acquisition, ≥30 ms.

The panels in Figure 1 are high-resolution, "bright" and "dark" false-color PL intensity images that are representative of the synchronized, whole-wire PL blinking phenomenon. These images were acquired with CCD integration times of 50 ms and a low excitation power of 7 W cm^{-2}. The two

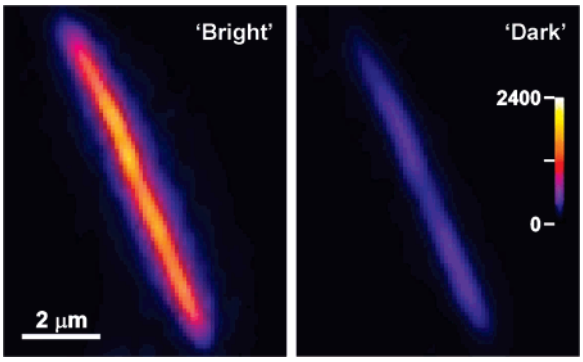

Figure 1. False-color PL images of a single ≈7 μm long, 9 nm diameter CdSe QW. The left panel shows an image of a bright event in which the PL signal from the QW uniformly increases by 6× in comparison to a dark event where the PL signal from the QW is significantly lower, right panel. The color scale represents the number of counts over the 50 ms integration bin. A movie of this QW showing synchronous-PL behavior is available in Supporting Information, Movie M1.

images have the same intensity scale and exhibit a nearly uniform factor of 6 change in PL intensity along the entire length of the ≈7 μm long QW. A real-time movie of the temporal evolution of the PL intensity for this CdSe QW is included in Supporting Information, Movie M1. This blinking is not observed within the >30 ms temporal resolution of the apparatus when illuminating with power densities >500 W cm^{-2}. Instead the QWs appear to be in a constant, bright state following an initial enhancement period.

The synchronous nature of the blinking is recognized by comparing the temporal dependences of the integrated PL intensity measured at numerous positions along a single QW. The image in Figure 2 represents a frame from a low-resolution movie, Movie M2 in Supporting Information, that was acquired with a temporal resolution of 30 ms. The integrated PL intensity measured at the opposite ends of a single whole-wire blinking QW, plotted as traces a and b, are identical with no observable phase lags in the intensity profiles and no significant differences in the intensities at any time. It is important to emphasize that there is usually no correlation between the PL fluctuations observed from one wire, traces a or b, with that of another blinking QW, trace c, recorded at the same time and under identical conditions. Furthermore, the abundant, dark QWs do not have PL intensity fluctuations that vary by more than a factor of 2, trace d, and the slight fluctuations do not correspond with the timing of those in the whole-wire blinking QWs. These observations suggest that the synchronous PL blinking along entire QWs does not result from changing experimental parameters, such as those from unstable illumination power densities.

For those QWs that exhibited synchronous, whole-wire PL blinking, we monitored the integrated intensity of a single QW as a function of time. The integrated PL intensity−time profile for a single CdSe QW is plotted in Figure 3a. The probability distributions for bright and dark events in whole-wire PL blinking QWs were calculated and fit in a similar manner as described by Kuno et al.[19] The QW is said to be in a bright state if the PL intensity is >2× the minimum

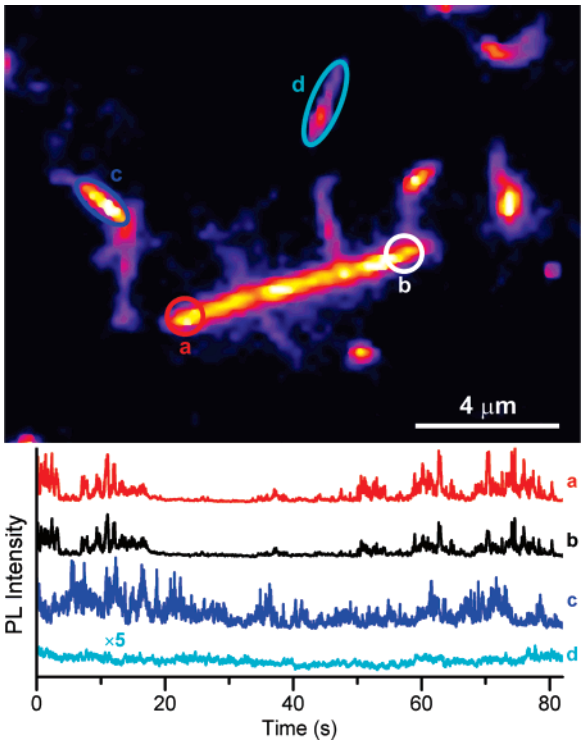

Figure 2. PL-intensity image of numerous CdSe QWs. The 14.19 × 13.55 μm^2 false-color PL image is a frame from movie M2 in Supporting Information. The graph shows the time dependence of the integrated PL intensity from the encircled regions. The PL intensity from each region was normalized to the peak intensity and then offset for clarity. The nearly identical PL intensity traces acquired from the opposite ends of the QW, traces a and b, indicate that the PL intensity fluctuates in a synchronous manner. There is no correlation for the PL intensity fluctuations in a and b with those of another blinking QW, trace c. Most of the QWs do not exhibit any significant fluctuations, and remain dark with small intensity fluctuations with time, d.

value, indicated by the red dashed line in Figure 3a, and in a dark state if it is below this threshold value. Both the bright- and dark-time probability distributions fit well to an inverse-power law, $P[t_{bright/dark}] = At^{m^{bright/dark}}$, as demonstrated in Figure 3b. Similar analyses were performed on 75 individual whole-wire-blinking CdSe QWs taken from five samples synthesized on different dates, and similar results were obtained. We observed no dependence of the bright- and dark-time statistics on illumination power over the range 7−100 W cm^{-2}. Consequently, we report average values for the power-law exponents of $m_{bright} = -1.6(2)$ and $m_{dark} = -1.6(2)$, Figure S1 in Supporting Information.

The probability distributions for the blinking QWs strongly resemble those for many types of QDs,[17,19,20] QRs,[27] and localized regions within QWs.[15] The power-law dependence of the PL intensity may be fortuitous or a consequence of the sampling intervals or analysis. In contrast, the normalized autocorrelation function, ACF, of the PL intensity versus time can directly reveal the randomness of the durations and frequency of the bright and dark events.[28] Representative experimental ACFs obtained for integrated PL intensity−time profiles with durations of 60, 300, and 2520 s are shown in Figure 3c as red, black, and blue curves, respectively. Each ACF remains relatively constant before quickly decreasing to unity as the time delay approaches the duration of the PL−time trace. These data indicate that there is no characteristic time scale governing the dynamics within the CdSe QWs.[28]

Even though the integrated PL intensity−time profiles and bright- and dark-time distributions of CdSe QWs that exhibit whole-wire blinking seem extremely similar to those of blinking core and core−shell semiconductor QDs,[16−20] there are a number of significant differences that suggest that the QD-blinking models and dynamics[10,17,21−26,29] would not apply to the blinking QWs. A high sensitivity of Φ to surface passivation for ensemble solutions of QWs[5,9,30−32] and colloidal QDs[33−36] has been demonstrated. This sensitivity is evidence of the strong role surface sites play in non-radiative recombination of photogenerated carriers. Since the QWs have significantly more surface area in comparison to the QDs of similar diameters, the QWs should have a larger number of dangling Se or Cd bonds that result from incomplete passivation of the semiconductor by the organic ligands. In partial support of this reasoning, we find that the highest obtainable Φ values of CdSe QWs suspended in solution are ≈0.2%. In contrast, the very high ensemble Φ values of QDs, approaching 100%,[33−36] suggest the presence of a fewer number of trap sites on QDs than on QWs.

Another significant difference between the blinking QWs and QDs is that the former have a weak, continuous-PL signal that is measured during dark periods. In contrast, no PL is detectable from QDs during off periods.[17,19] There is an induction period required before the blinking is detected in the QWs, whereas the blinking in QDs occurs immediately with illumination. Even after a QW is observed to be blinking, if the irradiation is turned off, an additional time period is needed before the onset of the synchronous-PL-intensity fluctuations are detected again when irradiation is resumed. Last, the statistics for QD blinking seem to be independent of illumination power density, whereas with power densities of >500 W cm^{-2} the blinking QWs appear to remain in a constant bright state.

We propose a new, simplistic model based on the filling of surface trap sites to explain the delocalized PL blinking observed in the CdSe QWs. Each time a photon is absorbed and a one-dimensional (1D) exciton or weakly bound electron−hole pair is formed, there is a probability that the exciton or one or both of the charges will become localized in a surface-trap site. The QD blinking data and models indicate that surface-trap sites can remain occupied for extended periods of time.[22] Thus, if the photon flux is high enough and the lifetimes of the excitons or charges within trap sites are long enough, it becomes possible for an exciton to be generated in a region along a QW, where trap sites have been photolytically filled, and the propensity for radiative recombination increases.

A full development of this model will be presented in a subsequent publication;[37] only a brief synopsis is given here. With the absorption of a photon having sufficient energy, the QW is excited from the ground state, $|g\rangle$, to above the first excitonic state, $|e\rangle$, as depicted in Figure 4. The excitation rate, k_{exc}, is based on the estimated absorption cross

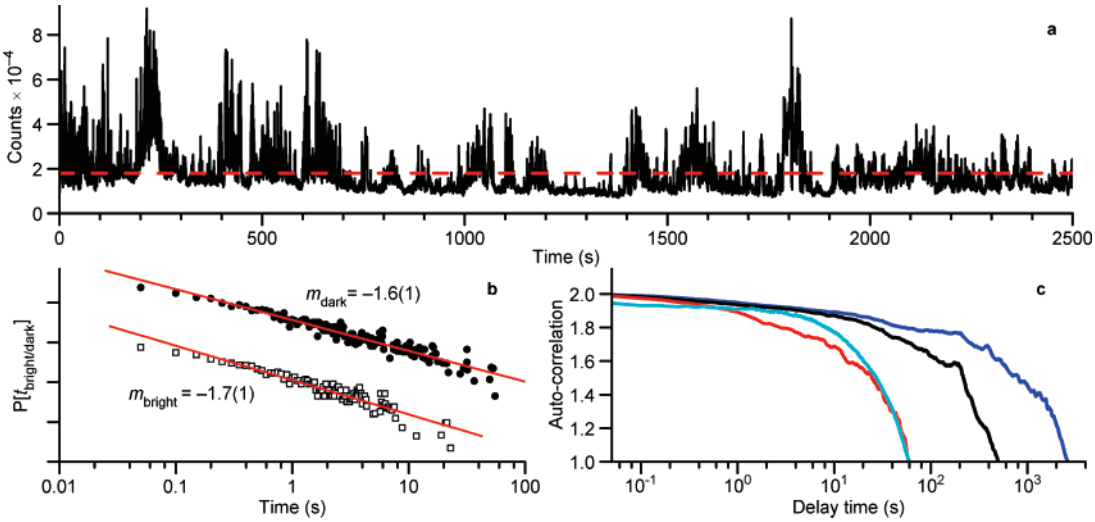

Figure 3. The integrated-PL intensity vs time profile for a single, blinking CdSe QW, panel a. The dashed, red line is the intensity threshold value used to differentiate between bright from dark events. log−log plots of the bright (open squares) and dark (black circles) time probability distributions are plotted in panel b. The dark data are vertically offset by an order of magnitude for clarity. The red lines represent linear fits to the log−log plots with the indicated exponential constants. Experimental autocorrelation functions of the time-dependent PL data for 60 s (red), 300 s (black), and 2520 s (blue) time traces. The autocorrelation function for a 60 s simulation is shown as the cyan trace.

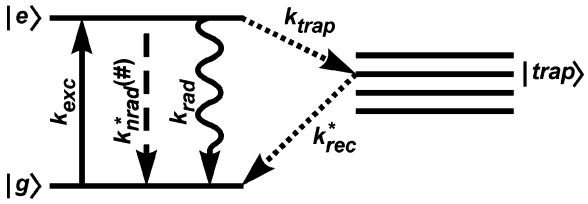

Figure 4. Schematic of the energetic states and pathways proposed to give rise to the observed synchronous-PL-intensity blinking along entire CdSe QWs. The rates for excitation, k_{exc}, radiative relaxation, k_{rad}, and trapping of both the electron and hole, k_{trap}, are fixed in the model, while the rate for nonradiative recombination, $k^*_{nrad}(\#)$, is dynamic with a dependence on the number of filled trap sites, #. The recombination of electrons and holes out of trap sites, k^*_{rec}, is dynamic and is based on a power-law distribution that is identical to that implemented for charge-trap emptying in QDs, ref 22.

section for the QWs[15] and a typical experimental power density. Upon absorption of a photon, a one-dimensional, 1D, exciton that is confined in the radial dimension and free along the length of the QW is generated. The 1D exciton, or electron−hole pair, may recombine radiatively, non-radiatively, or become localized in trap sites with respective rates of k_{rad}, $k^*_{nrad}(\#)$, and k_{trap}. The rate for radiative relaxation, k_{rad}, is constant and is set to $4 \times 10^8\ s^{-1} = (\tau)^{-1} = (2.5\ ns)^{-1}$. Simulations were performed with $\tau = 700$ ps and up to 10 ns, and no significant changes were noticeable in the data. For simplicity, we group the competing pathways for all nonradiative recombination into a single nonradiative rate, $k^*_{nrad}(\#)$. The value of $k^*_{nrad}(\#)$ is dynamic in the model with a dependence on the number of occupied trap sites, #, becoming smaller when the number of filled traps becomes large. The rate of exciton or electron and hole trapping, k_{trap}, is assumed to be small and is kept at a constant, low value. Since Auger relaxation will minimize the propensity for a significant buildup of charge within the core of a QW, the model assumes that either the exciton is trapped or the electron and hole are concurrently trapped, and individual electron or hole trapping is not considered. The rate for recombination of the excitons or electrons and holes out of trap sites, k^*_{rec}, is dynamic and is drawn from a power-law distribution with similar parameters as used by Verberk et al.[22] in simulations of core−shell QD blinking.

The PL quantum yield, $\Phi^*(\#) = k_{rad}/\{k_{rad} + k^*_{nrad}(\#) + k_{trap}\}$, will necessarily be dynamic in this model and depend predominantly on the number of and population in the long-lived trap sites, $|trap\rangle$. Since k_{trap} is small, especially in comparison to k_{rad} and $k^*_{nrad}(\#)$, the PL quantum yield is approximated as $\Phi^*(\#) = k_r/\{k_r + k^*_{nrad}(\#)\}$. It is this dynamic $\Phi^*(\#)$ that gives rise to the experimentally observed whole-wire, synchronous-PL-intensity fluctuations. Initially, the $\Phi^*(\#)$ of the QW is held near the solution-ensemble value and the estimate of Φ for the darker single QWs that do not exhibit synchronous-PL blinking, ≈0.50%. Only when nearly all of the trap sites become occupied does the $\Phi^*(\#)$ begin to increase significantly. Consequently, we chose to use a sigmoidal function for $\Phi^*(\#)$ with a significant increase occurring when ≈90% of the charge-trap sites are full.

Experimental and simulated PL intensity−time profiles for a single CdSe QW are shown in parts a and b of Figure 5, respectively. An integration-bin width of 50 ms was used in both panels. The simulation qualitatively compares to the experimental data in a number of significant ways. First, the significant background intensity observed experimentally is also present in the simulation. Second, the varying intensity of the bright events observed is also reproduced. The durations of the bright and dark events are comparable. The simulations also indicate an induction period during which a majority of the trap sites are filling prior to the onset of the PL blinking. The induction period is significantly shorter,

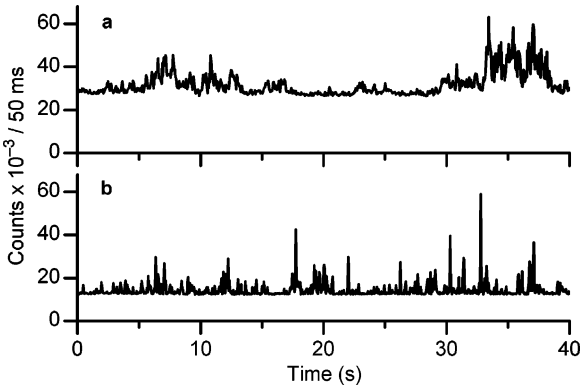

Figure 5. Experimental, a, and simulated, b, time dependence of the integrated-PL intensity for a single CdSe QW.

<1 s, than that observed experimentally but is very sensitive to the number of traps included, the irradiation power, and the shape of the PL quantum yield function.

Analysis of the time traces suggests further validity of the model. log−log plots of the simulated data indicate linear dependences on the durations for both bright and dark events.[37] The simulated dark events span 3 decades in time and 4 in probability, while the bright times span 2 decades in time and 3 in probability. Inverse power-law fits of the bright and dark simulated events yield exponents of −2.3(2) and −1.7(1), respectively. These values vary from simulation to simulation and on the bin times used. Even so, the power-law exponents are comparable to the average values obtained for the QWs, −1.6(2), for both the bright and dark events. The ACF of the simulated data, cyan line in Figure 3c, has a similar dependence on delay time as exhibited by the experimental ACFs. These trends are indicative of the nonergodic behavior of the QW blinking and add support to the simplistic model implemented. The agreement between the simulations and experimental data is achieved despite the identical treatment for the exciton-, electron-, and hole-trap sites, and the omission of the precise mechanisms for filling or emptying the trap sites and for nonradiative relaxation in the model.

In summary, our experiments reveal that a fraction of the CdSe QWs synthesized using the SLS method exhibit synchronous fluctuations in the PL intensity along the entire lengths of the QW. The absorption and PL spectroscopy of these QWs indicate that carrier-confinement energies scale according to a quantum-mechanical particle-in-an-infinitely-long-cylinder equation.[7−9] Since there is a finite probability that the photogenerated excitons or electron−hole pairs become trapped in long-lived, surface-trap sites, an appreciable number of these trap sites can become occupied with continuous irradiation. When this occurs, the Φ of the QW increases. The resultant, dynamic Φ values for single CdSe QWs are experimentally estimated to be as high as 20% when most of the trap sites are occupied, with the QW in a bright state, and as low as 0.2−0.5% otherwise.

These observations suggest that the SLS-synthetic method can produce QWs of sufficient quality for generation of 1D excitons. In the QWs synthesized, surface-trap sites that can quench these excitons are present. The significant jumps in the PL Φ along entire QWs indicate that when a majority of the sites become filled, the unperturbed nature of the 1D excitons is realized. While the proposed blinking model is simple, it does reproduce quite well the observed fluctuations in PL intensity. Furthermore, it is because of this synchronous blinking that the delocalized nature of the 1D excitons spanning micrometers in length is observed. These results also suggest that with proper passivation of the semiconductor QW surface, efficient transport of charge along the QWs should be possible, opening the way for their implementation in nanoelectronics and photovoltaics.

Acknowledgment. This work was funded by the National Science Foundation under Grant Number CHE-0518427, the David and Lucile Packard Foundation via a Fellowship in Science and Engineering, and the Center for Materials Innovation at Washington University in St. Louis.

Supporting Information Available: Synthesis, imaging, blinking analysis, QW size distribution, QW absorption spectra, and movies of blinking QWs. This material is available free of charge via the Internet at http://pubs.acs.org.

References

(1) Huynh, W. U.; Dittmer, J. J.; Alivisatos, A. P. *Science* **2002**, *295*, 2524.
(2) Huynh, W. U.; Dittmer, J. J.; Teclemariam, N.; Milliron, D. J.; Alivisatos, A. P.; Barnham, K. W. J. *Phys. Rev. B* **2003**, *67*, 115326.
(3) Pientka, M.; Wisch, J.; Boger, S.; Parisi, J.; Dyakonov, V.; Rogach, A.; Talapin, D.; Weller, H. *Thin Solid Films* **2004**, *451−452*, 48.
(4) Lieber, C. M. *MRS Bull.* **2003**, *28*, 486.
(5) Protasenko, V.; Bacinello, D.; Kuno, M. *J. Phys. Chem. B* **2006**, *110*, 25322.
(6) Snaith, H. J.; Whiting, G. L.; Sun, B.; Greenham, N. C.; Huck, W. T. S.; Friend, R. H. *Nano Lett.* **2005**, *5*, 1653.
(7) Yu, H.; Li, J.; Loomis, R. A.; Gibbons, P. C.; Wang, L.-W.; Buhro, W. E. *J. Am. Chem. Soc.* **2003**, *125*, 16168.
(8) Yu, H.; Li, J.; Loomis, R. A.; Wang, L.-W.; Buhro, W. E. *Nat. Mater.* **2003**, *2*, 517.
(9) Wang, F.; Dong, A.; Sun, J.; Tang, R.; Yu, H.; Buhro, W. E. *Inorg. Chem.* **2006**, *45*, 7511.
(10) Efros, A. L.; Rosen, M.; Kuno, M.; Nirmal, M.; Norris, D. J.; Bawendi, M. *Phys. Rev. B* **1996**, *57*, 4843.
(11) Slachmuylders, A. F.; Partoens, B.; Magnus, W.; Peters, F. M. *Phys. Rev. B* **2006**, *74*, 235321.
(12) Granot, E. *Phys. Rev. B* **2002**, *65*, 233101.
(13) Braun, W.; Bayer, M.; Forchel, A.; Schmitt, O. M.; Bányai, L.; Haug, H.; Filin, A. I. *Phys. Rev. B* **1998**, *57*, 12364.
(14) Jones, M.; Nedeljkovic, J.; Ellingson, R. J.; Nozik, A. J.; Rumbles, G. *J. Phys. Chem. B* **2003**, *107*, 11346.
(15) Protasenko, V. V.; Hull, K. L.; Kuno, M. *Adv. Mater.* **2005**, *17*, 2942.
(16) Nirmal, M.; Dabbousi, B. O.; Bawendi, M. G.; Macklin, J. J.; Trautman, J. K.; Harris, T. D.; Brus, L. E. *Nature* **1996**, *383*, 802.
(17) Shimizu, K. T.; Neuhauser, R. G.; Leatherdale, C. A.; Empedocles, S. A.; Woo, W. K.; Bawendi, M. G. *Phys. Rev. B* **2001**, *63*, 205316.
(18) Kuno, M.; Fromm, D. P.; Hamann, H. F.; Gallagher, A.; Nesbitt, D. J. *J. Chem. Phys.* **2000**, *112*, 3117.
(19) Kuno, M.; Fromm, D. P.; Hamann, H. F.; Gallagher, A.; Nesbitt, D. J. *J. Chem. Phys.* **2001**, *115*, 1028.
(20) Kuno, M.; Fromm, D. P.; Gallagher, A.; Nesbitt, D. J.; Micic, O. I.; Nozik, A. J. *Nano Lett.* **2001**, *1*, 557.
(21) Efros, A. L.; Rosen, M. *Phys. Rev. Lett.* **1997**, *78*, 1110.
(22) Verberk, R.; van Oijen, A. M.; Orrit, M. *Phys. Rev. B* **2002**, *66*, 233202.
(23) Kuno, M.; Fromm, D. P.; Johnson, S. T.; Gallagher, A.; Nesbitt, D. J. *Phys. Rev. B* **2003**, *67*, 125304.
(24) Margolin, G.; Barkai, E. *J. Chem. Phys.* **2004**, *121*, 1566.
(25) Tang, J.; Marcus, R. A. *Phys. Rev. Lett.* **2005**, *95*, 107401.

(26) Frantsuzov, P. A.; Marcus, R. A. *Phys. Rev. B* **2005**, *72*, 155321.
(27) Wang, S.; Querner, C.; Emmons, T.; Drndic, M.; Crouch, C. H. *J. Phys. Chem. B* **2006**, *110*, 23221.
(28) Messin, G.; Hermier, J. P.; Giacobino, E.; Desbiolles, P.; Dahan, M. *Opt. Lett.* **2001**, *26*, 1891.
(29) Chung, I.; Bawendi, M. G. *Phys. Rev. B* **2004**, *70*, 165304.
(30) Akamatsu, K.; Tsuruoka, T.; Nawafune, H. *J. Am. Chem. Soc.* **2005**, *127*, 1634.
(31) Berrettini, M. G.; Braun, G.; Hu, J. G.; Strouse, G. F. *J. Am. Chem. Soc.* **2004**, *126*, 7063.
(32) Querner, C.; Reiss, P.; Sadki, S.; Zagorska, M.; Pron, A. *Phys. Chem. Chem. Phys.* **2005**, *7*, 3210.
(33) de Mello Donegá, C.; Hickey, S. G.; Wuister, S. F.; Vanmaekelbergh, D.; Meijerink, A. *J. Phys. Chem. B* **2003**, *107*, 489.
(34) Peng, Z. A.; Peng, X. *J. Am. Chem. Soc.* **2001**, *123*, 183.
(35) Talapin, D. V.; Rogach, A. L.; Kornowski, A.; Haase, M.; Weller, H. *Nano Lett.* **2001**, *1*, 207.
(36) Wuister, S. F.; de Mello Donega, C.; Meijerink, A. *J. Phys. Chem. B* **2004**, *108*, 17393.
(37) Glennon, J. J.; Buhro, W. E.; Loomis, R. A. Submitted to *Chem. Phys. Lett.*

NL0714583